A MULTI-ORDER DISCONTINUOUS GALERKIN MONTE CARLO METHOD FOR HYPERBOLIC PROBLEMS WITH STOCHASTIC PARAMETERS

MOHAMMAD MOTAMED* AND DANIEL APPELÖ†

Abstract. We present a new multi-order Monte Carlo algorithm for computing the statistics of stochastic quantities of interest described by linear hyperbolic problems with stochastic parameters. The method is a non-intrusive technique based on a recently proposed high-order energy-based discontinuous Galerkin method for the second-order acoustic and elastic wave equations. The algorithm is built upon a hierarchy of degrees of polynomial basis functions rather than a mesh hierarchy used in multi-level Monte Carlo. Through complexity theorems and numerical experiments, we show that the proposed multi-order method is a valid alternative to the current multi-level Monte Carlo method for hyperbolic problems. Moreover, in addition to the convenience of working with a fixed mesh, which is desirable in many real applications with complex geometries, the multi-order method is particularly beneficial in reducing errors due to numerical dispersion in long-distance propagation of waves. The numerical examples verify that the multi-order approach is faster than the mesh-based multi-level approach for waves that traverse long distances.

Key words. Hyperbolic problems; Wave propagation; Stochastic parameters; Uncertainty quantification; Multi-level Monte Carlo; Discontinuous Galerkin; Multi-order Monte Carlo

AMS subject classifications.

1. Introduction.

Wave propagation problems are mathematically described by hyperbolic partial differential equations (PDEs). In real applications, such as seismology, acoustics, and electromagnetism, the problem is subject to uncertainty, due to the lack of knowledge (epistemic uncertainty) and/or intrinsic variabilities of the physical system (aleatoric uncertainty). For instance, in earthquake ground motion, both kinds of uncertainties are present due to the scarcity of measured soil parameters and inherent variations in the location of the focus and the intensity of seismic sources. To account for uncertainties, PDE models are often formulated in a probabilistic framework, where uncertain input parameters are described by stochastic fields, which can in turn be approximated by a finite number of random variables. A major problem is then the forward propagation of uncertainty, where uncertainties in the input parameters are propagated through the model to obtain information about uncertain output quantities of interest (QoIs).

The most popular method for propagating stochastic uncertainty in PDE models is Monte Carlo sampling [8], where sample statistics of output QoIs are computed from independent realizations drawn from the input probability distributions. While being very flexible and easy to implement, this technique features a very slow convergence rate. More recently, spectral approaches, such as stochastic Galerkin [9] and stochastic collocation [17, 19], have been proposed, which exploit the possible regularity that output QoIs might have with respect to the input parameters. This opens up the possibility to use deterministic approximations of the response function (i.e. the solution of the problem as a function of the input parameters) based on global polynomials. Such approximations are expected to yield a very fast convergence in

*Department of Mathematics and Statistics, University of New Mexico, 1 University of New Mexico, Albuquerque, NM 87131. motamed@math.unm.edu.

†Department of Mathematics and Statistics, University of New Mexico, 1 University of New Mexico, Albuquerque, NM 87131. appelo@math.unm.edu.

Funding: Supported in part by NSF Grant DMS-1319054. Any conclusions or recommendations expressed in this paper are those of the author and do not necessarily reflect the views of NSF.

the presence of high stochastic regularity.

Solutions to parametric hyperbolic PDEs are in general non-smooth with respect to the parameters, and therefore related stochastic QoIs are often not regular; see [15, 16, 4]. Consequently, spectral methods may not be applicable to stochastic hyperbolic problems, and Monte Carlo sampling needs to be employed. Several variants of Monte Carlo sampling have recently been proposed to accelerate the slow convergence of the Monte Carlo method. These recent methods include multi-level Monte Carlo (MLMC) [10, 6, 5, 7], multi-index Monte Carlo [11], quasi-Monte Carlo [12], and multi-level quasi Monte Carlo [13]. In the particular case of hyperbolic problems, multi-level Monte Carlo approaches have been developed [14, 18], based on finite volume and finite difference techniques.

In the present work, we will develop a new variant of Monte Carlo sampling, referred to as *multi-order Monte Carlo* (MOMC). Compared to multi-level Monte Carlo, the method has two new components: 1) it is based on a recently proposed energy-based discontinuous Galerkin method for deterministic hyperbolic problems [3, 2]; and 2) it is built upon a hierarchy of orders of discontinuous Galerkin basis functions rather than a mesh hierarchy used in multi-level Monte Carlo. The new method is particularly advantageous for dealing with wave propagation and non-smooth QoIs, because: a) the energy-based discontinuous Galerkin method is capable of accurately treating discontinuities in the PDE coefficients and the PDE data; b) the construction of an order hierarchy based on high-order schemes, such as discontinuous Galerkin, allows us to significantly reduce wave dispersion and produce smaller errors; c) the method uses a fixed mesh at all levels which is beneficial when waves propagate in complicated media where re-meshing is a cumbersome task. The third advantage is of practical importance for instance when the material parameters come from a Bayesian seismic tomography at fixed resolution. Through complexity theorems and numerical experiments, we will demonstrate that the proposed multi-order method is a valid alternative to the current multi-level Monte Carlo method for hyperbolic problems with rough parameters. Moreover, in addition to the convenience of working with a fixed mesh, which is desirable in many real applications with complex geometries, the multi-order method is particularly beneficial in reducing errors due to numerical dispersion in long-time propagating waves. The numerical examples verify that the multi-order approach is faster than the mesh-based multi-level approach for waves that traverse long distances. Note that the MOMC requires that p-refinement can be efficiently used, which is the case for the examples considered here.

The outline of the paper is as follows. In Section 2 we formulate the mathematical problem and briefly address the numerical treatment of the problem with relation to stochastic regularity. The energy-based discontinuous Galerkin solver is briefly reviewed in Section 3. In Section 4, we present an adaptation of the multi-level Monte Carlo algorithm to the elastic wave equations discretized by the discontinuous Galerkin method. The new multi-order Monte Carlo method is presented in Section 5. In Section 6 we perform some numerical examples that verify our theoretical results. Finally, we present our conclusions in Section 7.

2. Problem Statement.

In this section, we first present the mathematical formulation of the stochastic problem. We then address the numerical treatment of the problem with relation to stochastic regularity.

2.1. Mathematical formulation.

Let $D \subset \mathbb{R}^d$ be a compact d-dimensional spatial domain, where $d = 2, 3$. As the prototype model for wave propagation subject to uncertainty, we consider the following initial boundary value problem (IBVP) for

the elastic wave equation with stochastic parameters:

$$
\begin{array}{lll}
\varrho(\mathbf{x},\mathbf{y})\,\mathbf{u}_{tt}(t,\mathbf{x},\mathbf{y}) - \nabla\cdot\boldsymbol{\sigma}(\mathbf{u}(t,\mathbf{x},\mathbf{y})) = \mathbf{f}(t,\mathbf{x},\mathbf{y}), & \text{in} & [0,T]\times D\times\Gamma,\\
\mathbf{u}(0,\mathbf{x},\mathbf{y}) = \mathbf{g}_1(\mathbf{x},\mathbf{y}), \quad \mathbf{u}_t(0,\mathbf{x},\mathbf{y}) = \mathbf{g}_2(\mathbf{x},\mathbf{y}), & \text{on} & \{t=0\}\times D\times\Gamma,\\
\boldsymbol{\sigma}(\mathbf{u}(t,\mathbf{x},\mathbf{y}))\cdot\hat{\mathbf{n}} = \mathbf{0}, & \text{on} & [0,T]\times\partial D\times\Gamma,
\end{array}
\tag{1}
$$

where $\mathbf{u} = (u_1,\ldots,u_d)^\top \in \mathbb{R}^d$ is the real-valued displacement vector, $t\in[0,T]$ is the time, $\mathbf{x} = (x_1,\ldots,x_d)\in\mathbb{R}^d$ is the vector of spatial variables, $\mathbf{y} = (y_1,\ldots,y_N)\in\Gamma\subset\mathbb{R}^N$ is a random vector, representing the uncertainty in the problem, and $\hat{\mathbf{n}}$ denotes the outward unit normal to the boundary ∂D. We use the convention that ∇ represents the gradient operator with respect to the spatial variables $\mathbf{x}$. The stress tensor $\boldsymbol{\sigma}$ for isotropic materials reads

$$
\boldsymbol{\sigma}(\mathbf{u}) = \lambda(\mathbf{x},\mathbf{y})\,\nabla\cdot\mathbf{u}\,I + \mu(\mathbf{x},\mathbf{y})\,(\nabla\mathbf{u} + (\nabla\mathbf{u})^\top). \tag{2}
$$

The material parameters are the density ϱ and Lame's parameters λ and μ. The sources of uncertainty are the material parameters (ϱ,λ,μ), the force term $\mathbf{f}$, and the initial data, $\mathbf{g}_1,\mathbf{g}_2$, characterized by $N\in\mathbb{N}_+$ independent random variables $y_1,\ldots,y_N$ with a bounded joint probability density $\rho(\mathbf{y}) = \prod_{n=1}^N \rho_n(y_n) : \Gamma\to\mathbb{R}_+$.

We take the force term and initial data as

$$
\mathbf{f}\in\mathbf{L}^2((0,T);\mathbf{L}^2(D)\otimes\mathbf{L}^2_\rho(\Gamma)), \qquad \mathbf{g}_1\in\mathbf{H}^1(D)\otimes\mathbf{L}^2_\rho(\Gamma), \qquad \mathbf{g}_2\in\mathbf{L}^2(D)\otimes\mathbf{L}^2_\rho(\Gamma), \tag{3}
$$

where $\mathbf{L}^2_\rho$ is the Hilbert space of vector-valued stochastic functions with bounded second moments, $\mathbf{L}^2$ is the Hilbert space of square integrable vector-valued functions, and $\mathbf{H}^1$ is the Hilbert space of vector-valued functions whose first weak derivatives are square integrable. The notation $\otimes$ denotes the tensor product space of Hilbert spaces. We further assume that the data are compatible. Moreover, we assume that the material parameters are uniformly coercive and bounded:

$$
0 < \varrho_{min} \le \varrho(\mathbf{x},\mathbf{y}) \le \varrho_{max} < \infty, \quad \forall\,\mathbf{x}\in D, \quad \forall\,\mathbf{y}\in\Gamma, \tag{4a}
$$

$$
0 < \lambda_{min} \le \lambda(\mathbf{x},\mathbf{y}) \le \lambda_{max} < \infty, \quad \forall\,\mathbf{x}\in D, \quad \forall\,\mathbf{y}\in\Gamma, \tag{4b}
$$

$$
0 < \mu_{min} \le \mu(\mathbf{x},\mathbf{y}) \le \mu_{max} < \infty, \quad \forall\,\mathbf{x}\in D, \quad \forall\,\mathbf{y}\in\Gamma. \tag{4c}
$$

We note that assumption (4) is a natural assumption for elastic materials. We also note that in real applications, the material parameters and data are often not smooth. We have therefore made the minimal regularity assumptions (3)-(4) to account for more general wave propagation problems. The assumptions (3)-(4) guarantee that the problem (1) is well-posed: there exists a unique weak solution $\mathbf{u}\in\mathbf{C}^0([0,T];\mathbf{H}^1(D)\otimes\mathbf{L}^2_\rho(\Gamma))$ which depends continuously on the data; see [15, 16] for more details and proofs.

The ultimate goal is the prediction of statistics of the wave solution $\mathbf{u}$ or some physical quantities of interest (QoIs) related to the solution, such as

$$
\mathcal{Q}(\mathbf{y}) = \int_0^T \int_{D_Q\subseteq D} |L(\mathbf{u})|^2(t,\mathbf{x},\mathbf{y})\,d\mathbf{x}\,dt, \tag{5}
$$

where $L(\mathbf{u})$ may be a differential operator applied on $\mathbf{u}$, and $D_Q\subseteq D$ is a part of the computational domain. For instance, the cases where $L(\mathbf{u})$ is $\mathbf{u},\mathbf{u}_t$, and $\mathbf{u}_{tt}$ correspond to wave strength, kinetic energy, and Arias intensity, respectively.

2.2. Non-intrusive numerical methods and stochastic regularity. The goal of computations is to numerically approximate the statistical moments of the quantity (5). For instance, consider the first moment of the QoI and let $\mathcal{A}$ be its approximation:

$$\mathbb{E}[\mathcal{Q}] = \int_{\Gamma} \mathcal{Q}(\mathbf{y})\, \rho(\mathbf{y})\, d\mathbf{y} \;\approx\; \mathcal{A}.$$

Non-intrusive methods, such as Monte Carlo [8] and sparse stochastic collocation [19, 17, 15], are popular sample-based approaches that rely on solving a set of deterministic problems corresponding to a set of realizations. In a non-intrusive method, the approximation $\mathcal{A}$ involves two separate approximations: 1) the approximation of $\mathcal{Q}$, denoted by $\tilde{\mathcal{Q}}$; and 2) the approximation of the integral. The former needs a deterministic solver that computes $\tilde{\mathcal{Q}}$ at a set of M quadrature points, and the latter requires a quadrature rule, such as sample averages (in Monte Carlo) or Gauss or Clenshaw-Curtis quadrature (in stochastic collocation). Correspondingly, the total error in the approximation can be split into two parts:

$$\varepsilon := |\mathbb{E}[\mathcal{Q}] - \mathcal{A}| \leq \underbrace{|\mathbb{E}[\mathcal{Q}] - \mathbb{E}[\tilde{\mathcal{Q}}]|}_{\varepsilon_I} + \underbrace{|\mathbb{E}[\tilde{\mathcal{Q}}] - \mathcal{A}|}_{\varepsilon_{II}}.$$

The first error term ε_I corresponds to the discretization error in the deterministic solver, and the second error term ε_{II} is the quadrature error. We note that in Monte Carlo sampling, ε_{II} is a statistical error, as $\mathcal{A}$ is a statistical term.

In general, the choice of the numerical method strongly depends on the regularity of the mapping $\mathcal{Q} : \Gamma \to \mathbb{R}$, which in turn depends on the stochastic regularity of the wave solution $\mathbf{u}$, i.e. the regularity of $\mathbf{u}$ with respect to $\mathbf{y}$. In the presence of high stochastic regularity, sparse stochastic collocation exhibits fast convergence in the number of quadrature or collocation points and is preferable. However, if the QoI is not smooth in stochastic space, Monte Carlo sampling techniques must be employed. It is known that the solutions of hyperbolic problems, such as the IBVP (1) with the minimal assumptions (3)-(4), are not smooth in the stochastic space; see [15, 16, 4]. Consequently, the QoI (5) does not have stochastic regularity. We therefore need to employ MC-based sampling techniques. The most popular one is the classical Monte Carlo method. While being very flexible and easy to implement, this technique features a very slow convergence rate. More recently, several variants of Monte Carlo are proposed to accelerate the slow convergence of the Monte Carlo method, including multi-level Monte Carlo [10, 6, 5, 7], multi-index Monte Carlo [11], quasi-Monte Carlo [12], and multi-level quasi Monte Carlo [13]. In the particular case of hyperbolic problems, multi-level Monte Carlo approaches have been developed [14, 18], based on finite volume and finite difference techniques.

In the present work, we will develop a new variant of Monte Carlo sampling, which we call the multi-order Monte Carlo method. The method is based on a recently proposed energy-based discontinuous Galerkin method for deterministic hyperbolic problems [3] and is built upon a hierarchy of orders of basis functions rather than a mesh hierarchy used in multi-level Monte Carlo. In what follows, we will briefly review the deterministic solver in Section 3. We then present a multi-level and the new multi-order algorithms based on the energy-based discontinuous Galerkin method in Sections 4 and 5, respectively.

3. Deterministic solvers: energy based discontinuous Galerkin methods. In this section we briefly review the deterministic solver is the basis for our

multi-level and multi-order Monte Carlo methods. As we aim for arbitrary order of accuracy in space as well as in time we combine a new class of spatial dG discretization with Taylor series time-stepping.

3.1. Spatial discretization by an energy based discontinuous Galerkin method. Our spatial discretization is an direct application of the formulation described for general second order wave equations in [3] and for the elastic wave equation in [2]. Here we outline the spatial discretization for the special case of the scalar wave equation in one dimension and refer the reader to [3] for the general case. We note that an open source implementation of the method used for the example with the elastic wave equation in Section 6.2 is available, [1].

The energy of the scalar wave equation is

$$H(t) = \int_D \frac{v^2}{2} + G(x, u_x) dx,$$

where $G(x, u_x) = c^2(x)u_x^2/2$ is the potential energy density, v is the velocity or the time derivative of the displacement, $v = u_t$. The wave equation, written as a second order equation in space and first order in time then takes the form

$$u_t = v, \quad v_t = -\delta G,$$

where δG is the variational derivative of the potential energy

$$\delta G = -(G_{u_x})_x = -(c^2(x)u_x)_x.$$

For the continuous problem the change in energy is

$$\frac{dH(t)}{dt} = \int_D v v_t + u_t(c^2(x)u_x)_x \, dx = [u_t(c^2(x)u_x)]_{\partial D}, \tag{6}$$

where the last equality follows from integration by parts together with the wave equation. Now, a variational formulation that mimics the above energy identity can be obtained if the equation $v - u_t = 0$ is tested with the variational derivative of the potential energy. Let Ω_j be an element and $\Pi^s(\Omega_j)$ be the space of polynomials of degree s, then the variational formulation on that element is:

PROBLEM 1. *Find* $v^h \in \Pi^s(\Omega_j)$, $u^h \in \Pi^r(\Omega_j)$ *such that for all* $\psi \in \Pi^s(\Omega_j)$, $\phi \in \Pi^r(\Omega_j)$

$$\int_{\Omega_j} c^2 \phi_x \left(\frac{\partial u_x^h}{\partial t} - v_x^h \right) dx = [c^2 \phi_x \cdot n \left(v^* - v^h \right)]_{\partial \Omega_j}, \tag{7}$$

$$\int_{\Omega_j} \psi \frac{\partial v^h}{\partial t} + c^2 \psi_x \cdot u_x^h \, dx = [\psi \left(c^2 \, u_x \right)^*]_{\partial \Omega_j}. \tag{8}$$

Let $[[f]]$ and $\{f\}$ denote the jump and average of a quantity f at the interface between two elements, then, choosing the numerical fluxes as

$$v^* = \{v\} - \tau_1 [[c^2 \, u_x]]$$
$$(c^2 \, u_x)^* = \{c^2 \, u_x\} - \tau_2 [[v]],$$

will yields a contribution $-\tau_1([[c^2 \, u_x]])^2 - \tau_2([[v]])^2$ from each element face to the change of the discrete energy

$$\frac{dH^h(t)}{dt} = \frac{d}{dt} \sum_j \int_{\Omega_j} \frac{(v^h)^2}{2} + G(x, u_x^h).$$

Physical boundary conditions can also be handled be appropriate specification of the numerical fluxes, see [3] for details. The above variational formulation and choice of numerical fluxes results in an energy identity similar to (6). However, as the energy is invariant to certain transformations the variational problem does not fully determine the time derivatives of u^h on each element and independent equations must be introduced. In this case there is one invariant and an independent equation is $\int_{\Omega_j} \left(\frac{\partial u^h}{\partial t} - v^h \right) = 0$. For the general case and for the elastic wave equation see [3] and [2].

Here we always choose $\tau_i > 0$ (so called upwind or Sommerfeld fluxes) which typically result in methods that are $q = r + 1$ order accurate in space.

3.2. Taylor series time-stepping. In order to match the order of accuracy in space and time we employ Taylor series time-stepping. Assuming that all the degrees of freedom have been assembled into a vector $\mathbf{w}$ we can write the semi-discrete method as $\mathbf{w}_t = A\mathbf{w}$ with A being a matrix representing the spatial discretization. Assuming we know the discrete solution at the time t_n we can advance it to the next time step $t_{n+1} = t_n + \Delta t$ by the simple formula

$$\begin{aligned} \mathbf{w}(t_n + \Delta t) &= \mathbf{w}(t_n) + \Delta t\, \mathbf{w}_t(t_n) + \frac{(\Delta t)^2}{2!} \mathbf{w}_{tt}(t_n) \dots \\ &= \mathbf{w}(t_n) + \Delta t\, A\, \mathbf{w}(t_n) + \frac{(\Delta t)^2}{2!} A^2\, \mathbf{w}(t_n) \dots \end{aligned}$$

The stability domain of the Taylor series which truncates at time derivative number N_{T} includes the imaginary axis if $\mathrm{mod}(N_{\mathrm{T}}, 4) = 3$ or $\mathrm{mod}(N_{\mathrm{T}}, 4) = 0$. However as we use a slightly dissipative spatial discretization the spectrum of our discrete operator will be contained in the stability domain of all sufficiently large choices of N_{T} (i.e. the N_{T} should not be smaller than the spatial order of approximation). Note also that the stability domain grows linearly with the number of terms. We thus consider methods based on the combination of the spatial dG discretization of order q combined with a Taylor series with $N_{\mathrm{T}} = 2\lceil \frac{q}{2} \rceil$, where $\lceil . \rceil$ is the ceiling operator. This yields methods of order of accuracy $\min(q, N_{\mathrm{T}})$. We note that we will use this choice of N_{T} for both multi-level and multi-order based MC methods in Sections 4 and 5. We also note that below we exclusively use the mesh size h as a discretization parameter, but that it is directly proportional to the temporal discretization size Δt, through the CFL condition.

4. A multi-level discontinuous Galerkin Monte Carlo method. In this section, we present an adaptation of the multi-level Monte Carlo algorithm to the elastic wave equations discretized by the dG method. We note that although MLMC algorithms for hyperbolic PDEs based on finite difference and finite volume methods have already been introduced [14, 18], the analysis of MLMC based on the dG method is different and results in new theoretical results. It also serves as a basis for developing the new MOMC method.

We follow [10] and build a mesh hierarchy with a decreasing sequence of mesh sizes $h_0 > h_1 > \ldots > h_L$. For instance we take

$$h_l = h_0\, \beta^{-l}, \qquad l = 0, 1, \ldots, L, \qquad \beta \geq 2. \tag{9}$$

We denote by $\mathcal{Q}_l$, the discretization of $\mathcal{Q}$ by the dG method on the mesh at the l-th

level with mesh size h_l. We then use a telescoping sum formulation and write

$$\mathbb{E}[\mathcal{Q}] = \mathbb{E}[\mathcal{Q} - \mathcal{Q}_L] + \mathbb{E}[\mathcal{Q}_L], \qquad \mathbb{E}[\mathcal{Q}_L] = \mathbb{E}[\mathcal{Q}_0] + \sum_{l=1}^{L} \mathbb{E}[\mathcal{Q}_l - \mathcal{Q}_{l-1}].$$

The MLMC estimator approximates the terms in the telescoping sum by sample averages

$$\mathcal{A}_{\text{MLMC}} = \frac{1}{M_0} \sum_{m_0=1}^{M_0} \mathcal{Q}_0^{(m_0)} + \sum_{l=1}^{L} \frac{1}{M_l} \sum_{m_l=1}^{M_l} (\mathcal{Q}_l^{(m_l)} - \mathcal{Q}_{l-1}^{(m_l)}). \tag{10}$$

Here, $\mathcal{Q}_l^{(m_l)} := \mathcal{Q}_l(\mathbf{y}^{(m_l)})$, with $m_l = 1, \ldots, M_l$, are M_l realizations of $\mathcal{Q}_l$ corresponding to M_l independent samples $\{\mathbf{y}^{(m_l)}\}_{m_l=1}^{M_l}$ of the random vector $\mathbf{y}$. The total MLMC error reads

$$\varepsilon_{\text{MLMC}} = |\mathbb{E}[\mathcal{Q}] - \mathcal{A}_{\text{MLMC}}| \leq \underbrace{|\mathbb{E}[\mathcal{Q} - \mathcal{Q}_L]|}_{\varepsilon_I} + \underbrace{|\mathbb{E}[\mathcal{Q}_L] - \mathcal{A}_{\text{MLMC}}|}_{\varepsilon_{II}}.$$

The first error term ε_I is the discretization error in the dG solver, or the weak error, which satisfies

$$\varepsilon_I \leq c_1 \, h_L^{q_1}, \qquad \forall \, \mathbf{y} \in \Gamma, \tag{11}$$

where q_1 is related to the order q of the dG method, and c_1 is a positive constant which may depend on $\mathcal{Q}$. Moreover, by the central limit theorem, the statistical error ε_{II} satisfies

$$\varepsilon_{II} \lesssim c_\alpha \sqrt{\mathbb{V}[\mathcal{A}_{\text{MLMC}}]} = c_\alpha \sqrt{\frac{\mathbb{V}[\mathcal{Q}_0]}{M_0} + \sum_{l=1}^{L} \frac{\mathbb{V}[\mathcal{Q}_l - \mathcal{Q}_{l-1}]}{M_l}} =: c_\alpha \sqrt{\sum_{l=0}^{L} \frac{V_l}{M_l}}, \tag{12}$$

where $V_0 = \mathbb{V}[\mathcal{Q}_0]$ and $V_l = \mathbb{V}[\mathcal{Q}_l - \mathcal{Q}_{l-1}]$ for $l \geq 1$. Here, the notation $\lesssim$ is interpreted in the following statistical sense:

$$P\Big(\varepsilon_{II} \leq c_\alpha \sqrt{\sum_{l=0}^{L} \frac{V_l}{M_l}} \Big) \to 2\,\phi(c_\alpha) - 1, \qquad \text{as} \quad M_l \to \infty, \tag{13}$$

where P is a probability measure, and $\phi(c_\alpha) = \int_{-\infty}^{c_\alpha} \frac{1}{\sqrt{2\,\pi}} \exp(-\tau^2/2)\, d\tau$ is the cumulative density function (CDF) of a standard normal random variable. The larger the confidence parameter $c_\alpha > 0$, the higher the probability that $\varepsilon_{II} \leq c_\alpha \sqrt{\sum_{l=0}^{L} V_l/M_l}$ holds. We further note that we have the strong error

$$\mathbb{V}[\mathcal{Q} - \mathcal{Q}_l] \leq \mathbb{E}[(\mathcal{Q} - \mathcal{Q}_l)^2] \leq c_2 \, h_l^{q_2}, \qquad \forall \, \mathbf{y} \in \Gamma. \tag{14}$$

4.1. Numerical algorithm. An error-complexity analysis is needed to optimally select the computational parameters, including the number of samples at different levels $\{M_l\}_{l=0}^{L}$, and the final level L. We introduce a splitting parameter θ and write

$$\varepsilon_{\text{MLMC}} \leq \varepsilon_I + \varepsilon_{II} \lesssim (1-\theta)\, \varepsilon_{\text{TOL}} + \theta \, \varepsilon_{\text{TOL}}, \qquad \theta \in (0,1),$$

where the errors ε_I and ε_{II} are given by (11) and (12), respectively. Moreover, noting that the cost of computing $\mathcal{Q}_l^{(m_l)} - \mathcal{Q}_{l-1}^{(m_l)}$ in the MLMC estimator (10) is dominated by the cost of computing $\mathcal{Q}_l^{(m_l)}$, which is $W_l \propto h_l^{-\gamma_1}$, the total computational cost of MLMC reads

$$W_{\text{MLMC}} \propto \sum_{l=0}^{L} M_l \, W_l, \qquad W_l \propto h_l^{-\gamma_1}.$$

Here, $\gamma_1 = d + 1 \geq 2$ is the space-time dimension and determines the number of degrees of freedom in the deterministic solver. We then take the following iterative strategy, consisting of two main steps:

1. Optimal number of samples. We obtain the optimal number of samples at different levels by minimizing the total computational cost W_{MLMC} subject to the accuracy constraint $\varepsilon_{II} \lesssim \theta \, \varepsilon_{\text{TOL}}$. Following the standard approach in MLMC [10], we use the method of Lagrange multipliers. With the Lagrangian

$$\mathcal{L}(M_l, \nu) := \sum_{l=0}^{L} M_l \, W_l + \nu \, \Big(\sum_{l=0}^{L} \frac{V_l}{M_l} - \big(\frac{\theta \, \varepsilon_{\text{TOL}}}{c_\alpha}\big)^2\Big),$$

and the optimality equations $\partial_{M_l} \mathcal{L} = \partial_\nu \mathcal{L} = 0$, we obtain

$$M_l = \Big\lceil \big(\frac{\theta \, \varepsilon_{\text{TOL}}}{c_\alpha}\big)^{-2} \sqrt{\frac{V_l}{W_l}} \sum_{\ell=0}^{L} \sqrt{V_\ell \, W_\ell} \Big\rceil, \qquad W_l \propto h_l^{-\gamma_1}. \tag{15}$$

2. Stopping criterion. We start with $L = 2$ and iteratively add levels until $\varepsilon_I \leq (1 - \theta) \, \varepsilon_{\text{TOL}}$ is achieved. To find a practical stopping criterion, we start by writing

$$\mathbb{E}[\mathcal{Q} - \mathcal{Q}_L] = \sum_{l=L+1}^{\infty} \mathbb{E}[\mathcal{Q}_l - \mathcal{Q}_{l-1}] = \mathbb{E}[\mathcal{Q}_L - \mathcal{Q}_{L-1}] \sum_{l=L+1}^{\infty} \frac{\mathbb{E}[\mathcal{Q}_l - \mathcal{Q}_{l-1}]}{\mathbb{E}[\mathcal{Q}_L - \mathcal{Q}_{L-1}]}. \tag{16}$$

Assuming $|\mathbb{E}[\mathcal{Q}_l - \mathcal{Q}_{l-1}]| \approx c \, h_l^{q_1}$, we have

$$\frac{|\mathbb{E}[\mathcal{Q}_l - \mathcal{Q}_{l-1}]|}{|\mathbb{E}[\mathcal{Q}_L - \mathcal{Q}_{L-1}]|} \approx \frac{h_l^{q_1}}{h_L^{q_1}} = \frac{h_0^{q_1} \, \beta^{-l \, q_1}}{h_0^{q_1} \, \beta^{-L \, q_1}} = \beta^{(L-l) \, q_1}.$$

Hence

$$\varepsilon_I = |\mathbb{E}[\mathcal{Q} - \mathcal{Q}_L]| \leq |\mathbb{E}[\mathcal{Q}_L - \mathcal{Q}_{L-1}]| \sum_{k=1}^{\infty} \beta^{-k \, q_1} = \frac{1}{\beta^{q_1} - 1} \, |\mathbb{E}[\mathcal{Q}_L - \mathcal{Q}_{L-1}]|,$$

where the last equality follows from the geometrical series $\sum_{k=0}^{\infty} (\beta^{-q_1})^k = \frac{1}{1-\beta^{-q_1}}$, since $\beta^{-q_1} < 1$. Consequently, the condition we use to add levels in the numerical algorithm is

$$\max_{j \in \{0,1,2\}} \frac{\beta^{-j \, q_1}}{\beta^{q_1} - 1} \, \big|\mathbb{E}[\mathcal{Q}_{L-j} - \mathcal{Q}_{L-j-1}]\big| \leq (1 - \theta) \, \varepsilon_{\text{TOL}}. \tag{17}$$

This criterion will ensure that the deterministic error approximated by an extrapolation from either of the three finest meshes is within the desired range.

Now, assuming that we have made the assignment $L \leftarrow L+1$, we note that in order to compute the number of samples by (15), we need to compute the variances $\{V_l\}_{l=0}^{L}$. Setting $\mathcal{Q}_{-1}^{(m)} = 0$, the variances are approximated by

$$V_l \approx \frac{1}{M_l} \sum_{m=1}^{M_l} \left(\left(\mathcal{Q}_l^{(m)} - \mathcal{Q}_{l-1}^{(m)} \right)^2 - \bar{G}_l^2 \right), \qquad \bar{G}_l \approx \frac{1}{M_l} \sum_{m=1}^{M_l} \left(\mathcal{Q}_l^{(m)} - \mathcal{Q}_{l-1}^{(m)} \right), \tag{18}$$

where $\{M_l\}_{l=0}^{L}$ are the available number of samples in previous iterations. When a new level L is added, the variance at the new level V_L cannot be approximated by (18), since the number of samples at the new level is not known. In this case, thanks to the strong error estimate (14), assuming $V_l = \mathbb{V}[\mathcal{Q}_l - \mathcal{Q}_{l-1}] \approx c\, h_l^{q_2}$, we first approximate V_L in terms of the variance at the previous level V_{L-1} by

$$V_L \approx \beta^{-q_2}\, V_{L-1}, \tag{19}$$

and then update the number of samples $\{M_l\}_{l=0}^{L}$ including the number of samples at the new level by (15). The expected values $\mathbb{E}[\mathcal{Q}_{L-j} - \mathcal{Q}_{L-j-1}]$ in (17), with $j = 0, 1, 2$, are also approximated by $\bar{G}_{L-j}$ in (18).

The MLMC algorithm is outlined in Algorithm 1.

Algorithm 1 MLMC algorithm

Start with $L = 2$, and generate a mesh hierarchy $\{h_l\}_{l=0}^{L}$ by (9).

Choose an initial set $\{M_l\}_{l=0}^{L}$ of samples.

loop

Approximate $\{V_l\}_{l=0}^{L}$ by (18).

Update the optimal number of samples $\{M_l\}_{l=0}^{L}$ by (15).

if (17) is satisfied

Compute $\mathcal{A}_{\text{MLMC}}$ by (10) and terminate the loop.

else

Set $L := L+1$ and $h_L = h_0\, \beta^{-L}$.

Approximate V_L by (19) and compute $\{M_l\}_{l=0}^{L}$ by (15).

end if

end loop

If it is possible to establish bounds on the strong and weak error and the work at each level, the complexity of Algorithm 1 is guaranteed by the following theorem.

THEOREM 1. *Consider a mesh hierarchy $h_l = h_0\, \beta^{-l}$, with $\beta \geq 2$, and let $\mathcal{Q}_l$ be the q-th order accurate dG approximation of $\mathcal{Q}$ on a mesh with mesh size h_l. If there are positive constants $c_1, c_2, c_3, \gamma_1 > 0$ such that*

$$\begin{aligned} &(A1) \quad |\mathbb{E}[\mathcal{Q} - \mathcal{Q}_l]| \leq c_1\, h_l^{q_1}, && q_1 \geq \gamma_1/2, \\ &(A2) \quad \mathbb{V}[\mathcal{Q} - \mathcal{Q}_l] \leq \mathbb{E}[|\mathcal{Q} - \mathcal{Q}_l|^2] \leq c_2\, h_l^{q_2}, && q_2 > \gamma_1, \\ &(A3) \quad W_l \leq c_3\, h_l^{-\gamma_1}, \end{aligned}$$

then, for any $\varepsilon_{TOL} < e^{-1}$, there exists an $L \in \mathbb{N}$ and a sequence $\{M_l\}_{l=0}^{L}$ such that the estimator $\mathcal{A}_{MLMC}$ has an error $\varepsilon_{MLMC} \lesssim \varepsilon_{TOL}$ with a computational cost proportional to ${\varepsilon_{TOL}}^{-2}$.

Proof. By writing $V_l = \mathbb{V}[\mathcal{Q}_l - \mathcal{Q}_{l-1}] = \mathbb{V}[\mathcal{Q} - \mathcal{Q}_{l-1}] - \mathbb{V}[\mathcal{Q} - \mathcal{Q}_l]$ and using the triangular inequality and *(A2)*, we get

$$V_l \leq c\, h_l^{q_2}, \qquad c = c_2(1 + \beta^{q_2} + 2\,\beta^{q_2/2}). \tag{20}$$

Moreover, by minimizing $\mathbb{V}[\mathcal{A}_{\text{MLMC}}]$, or equivalently minimizing ε_{II}, for a fixed computational cost W_{MLMC}, we obtain from *(A3)* and (20):

$$M_l \propto \sqrt{\frac{V_l}{W_l}} \propto h_l^{(\gamma_1+q_2)/2}. \tag{21}$$

We follow [10] and select L to be

$$L = \left\lceil \frac{\log(2c_1\, h_0^{q_1}\, {\varepsilon_{\text{TOL}}}^{-1})}{q_1\, \log\beta} \right\rceil.$$

We therefore have

$$\frac{1}{2}\,\varepsilon_{\text{TOL}}\,\beta^{-q_1} < c_1\, h_L^{q_1} \leq \frac{1}{2}\,\varepsilon_{\text{TOL}}. \tag{22}$$

By the right inequality in (22) and *(A1)*, the deterministic error is bounded by

$$\varepsilon_I \leq \frac{1}{2}\,\varepsilon_{\text{TOL}}. \tag{23}$$

Moreover, since $h_l = \beta^{L-l}\, h_L$, we have

$$\sum_{l=0}^{L} h_l^{-\gamma_1} = h_L^{-\gamma_1} \sum_{l=0}^{L} \beta^{-\gamma_1\, l} \leq h_L^{-\gamma_1} \sum_{l=0}^{\infty} \beta^{-\gamma_1\, l} = h_L^{-\gamma_1}\, \frac{\beta^{\gamma_1}}{\beta^{\gamma_1} - 1}.$$

Now, by the left inequality in (22) we have $h_L^{-\gamma_1} < (2c_1/\varepsilon_{\text{TOL}})^{\gamma_1/q_1}\, \beta^{\gamma_1}$, thus

$$\sum_{l=0}^{L} h_l^{-\gamma_1} \leq \frac{\beta^{2\gamma_1}}{\beta^{\gamma_1} - 1}\, (2c_1)^{\gamma_1/q_1}\, {\varepsilon_{\text{TOL}}}^{-\gamma_1/q_1},$$

and since $\varepsilon_{\text{TOL}} < e^{-1}$ and $\gamma_1/q_1 \leq 2$, then ${\varepsilon_{\text{TOL}}}^{-\gamma_1/q_1} \leq {\varepsilon_{\text{TOL}}}^{-2}$, and hence

$$\sum_{l=0}^{L} h_l^{-\gamma_1} \leq \frac{\beta^{2\gamma_1}}{\beta^{\gamma_1} - 1}\, (2c_1)^{\gamma_1/q_1}\, {\varepsilon_{\text{TOL}}}^{-2}. \tag{24}$$

Now, motivated by (21), we set

$$M_l = \left\lceil \frac{4\,{\varepsilon_{\text{TOL}}}^{-2}\, c\, c_\alpha^2\, h_0^{(q_2-\gamma_1)/2}}{1 - \beta^{-(q_2-\gamma_1)/2}}\, h_l^{(\gamma_1+q_2)/2} \right\rceil, \tag{25}$$

which gives

$$\frac{c\, c_\alpha^2}{M_l} \leq \frac{1}{4}\, {\varepsilon_{\text{TOL}}}^{2}\, h_0^{-(q_2-\gamma_1)/2}\, (1 - \beta^{-(q_2-\gamma_1)/2})\, h_l^{-(\gamma_1+q_2)/2}.$$

Then, by (20) we have

$$c_\alpha^2 \sum_{l=0}^{L} \frac{V_l}{M_l} \leq \sum_{l=0}^{L} \frac{c\, c_\alpha^2}{M_l} h_l^{q_2} \leq \frac{1}{4} {\varepsilon_{\text{TOL}}}^2 h_0^{-(q_2-\gamma_1)/2} (1-\beta^{-(q_2-\gamma_1)/2}) \sum_{l=0}^{L} h_l^{(q_2-\gamma_1)/2}.$$

Moreover, we have

$$\sum_{l=0}^{L} h_l^{(q_2-\gamma_1)/2} = h_0^{(q_2-\gamma_1)/2} \sum_{l=0}^{L} \left(\beta^{-(q_2-\gamma_1)/2}\right)^l < \frac{h_0^{(q_2-\gamma_1)/2}}{1-\beta^{-(q_2-\gamma_1)/2}}. \tag{26}$$

Hence, the statistical error is bounded by

$$\varepsilon_{II} \lesssim c_\alpha \sqrt{\sum_{l=0}^{L} \frac{V_l}{M_l}} \leq \frac{1}{2} \varepsilon_{\text{TOL}}. \tag{27}$$

By (23) and (27), the total error reads $\varepsilon_{\text{MLMC}} \lesssim \varepsilon_{\text{TOL}}$. It is left to show that the computational cost is proportional to ${\varepsilon_{\text{TOL}}}^{-2}$. By (25), we have

$$M_l < \frac{4\, {\varepsilon_{\text{TOL}}}^{-2}\, c\, c_\alpha^2\, h_0^{(q_2-\gamma_1)/2}}{1-\beta^{-(q_2-\gamma_1)/2}} h_l^{(\gamma_1+q_2)/2} + 1.$$

Hence, by *(A3)*, the computational cost reads

$$\begin{aligned} W_{\text{MLMC}} &= \sum_{l=0}^{L} M_l\, W_l \leq c_3 \sum_{l=0}^{L} M_l h_l^{-\gamma_1} \\ &< c_3 \sum_{l=0}^{L} \left(\frac{4\, {\varepsilon_{\text{TOL}}}^{-2}\, c\, c_\alpha^2\, h_0^{(q_2-\gamma_1)/2}}{1-\beta^{-(q_2-\gamma_1)/2}} h_l^{(q_2-\gamma_1)/2} + h_l^{-\gamma_1} \right). \end{aligned}$$

Eventually, by (26) and (24), we obtain

$$W_{\text{MLMC}} < c_{\text{W}}\, {\varepsilon_{\text{TOL}}}^{-2}, \quad c_{\text{W}} = 4\, c_3\, c\, c_\alpha^2\, h_0^{q_2-\gamma_1} (1-\beta^{-(q_2-\gamma_1)/2})^{-2} + c_3\, (2\, c_1)^{\gamma_1/q_1} \frac{\beta^{2\,\gamma_1}}{\beta^{\gamma_1}-1}.$$

This completes the proof. ∎

Note that for the sake of brevity we considered only the special case $\theta = 1/2$ in Theorem 1 but that it can be extended to the case of a general θ by tracking the splitting of the error in the proof.

5. A multi-order discontinuous Galerkin Monte Carlo method. In this section, we describe the new MOMC algorithm and present error and convergence analysis.

The new algorithm will first construct a fixed mesh, with a mesh size h, and build an order hierarchy with an increasing sequence of degrees of polynomial basis functions, or equivalently a sequence of dG orders $q_0 < q_1 < \ldots, < q_L$. For instance we take

$$q_l = q_0 + \beta\, l, \qquad l = 0, 1, \ldots, L, \qquad q_0 \geq 1, \qquad \beta \geq 1. \tag{28}$$

Denote by Q_l the approximation of Q by a q_l-th order dG on the fixed mesh. Using the same telescoping sum formulation as in MLMC and approximating the terms by sample averages, we write the MOMC estimator as

$$\mathcal{A}_{\text{MOMC}} = \frac{1}{M_0}\sum_{m_0=1}^{M_0} \mathcal{Q}_0^{(m_0)} + \sum_{l=1}^{L} \frac{1}{M_l}\sum_{m_l=1}^{M_l} (\mathcal{Q}_l^{(m_l)} - \mathcal{Q}_{l-1}^{(m_l)}). \tag{29}$$

Here, $\mathcal{Q}_l^{(m_l)} := \mathcal{Q}_l(\mathbf{y}^{(m_l)})$, is one realization of $\mathcal{Q}_l$ corresponding to a sample $\mathbf{y}^{(m_l)}$ of the random vector $\mathbf{y}$. The total MOMC error reads

$$\varepsilon_{\text{MOMC}} = |\mathbb{E}[\mathcal{Q}] - \mathcal{A}_{\text{MOMC}}| \leq \underbrace{|\mathbb{E}[\mathcal{Q} - \mathcal{Q}_L]|}_{\varepsilon_I} + \underbrace{|\mathbb{E}[\mathcal{Q}_L] - \mathcal{A}_{\text{MOMC}}|}_{\varepsilon_{II}}.$$

The first error term ε_I is the discretization error in the dG solver,

$$\varepsilon_I \leq c_1\, h^{q_{1L}}, \qquad q_{1L} := \kappa_1\, q_L, \qquad \forall\, \mathbf{y} \in \Gamma, \tag{30}$$

where $\kappa_1 > 0$ is related to the convergence of the dG solver in approximating $\mathbb{E}[\mathcal{Q}]$. The statistical error ε_{II}, interpreted in the statistical sense similar to (13), satisfies

$$\varepsilon_{II} \lesssim c_\alpha \sqrt{\mathbb{V}[\mathcal{A}_{\text{MOMC}}]} = c_\alpha \sqrt{\frac{\mathbb{V}[\mathcal{Q}_0]}{M_0} + \sum_{l=1}^{L} \frac{\mathbb{V}[\mathcal{Q}_l - \mathcal{Q}_{l-1}]}{M_l}} =: c_\alpha \sqrt{\sum_{l=0}^{L} \frac{V_l}{M_l}}. \tag{31}$$

The strong error also satisfies

$$\mathbb{V}[\mathcal{Q} - \mathcal{Q}_l] \leq \mathbb{E}[(\mathcal{Q} - \mathcal{Q}_l)^2] \leq c_2\, h^{q_{2l}}, \qquad q_{2l} = \kappa_2\, q_l, \qquad \forall\, \mathbf{y} \in \Gamma, \tag{32}$$

where $\kappa_2 > 0$ is related to the convergence of the dG solver in approximating $\mathbb{V}[\mathcal{Q}]$.

5.1. Numerical algorithm. Similar to MLMC, an error-complexity analysis is needed to optimally select the computational parameters. We split the total error by introducing a splitting parameter θ and write

$$\varepsilon_{\text{MOMC}} \leq \varepsilon_I + \varepsilon_{II} \lesssim (1-\theta)\,\varepsilon_{\text{TOL}} + \theta\,\varepsilon_{\text{TOL}}, \qquad \theta \in (0,1),$$

where the errors ε_I and ε_{II} are given by (30) and (31), respectively. Moreover, noting that the cost of computing $\mathcal{Q}_l^{(m_l)} - \mathcal{Q}_{l-1}^{(m_l)}$ in the MOMC estimator (29) is dominated by the cost of computing $\mathcal{Q}_l^{(m_l)}$, which is $W_l \propto q_l^{\gamma_2}$, the total computational cost of MOMC reads

$$W_{\text{MOMC}} \propto \sum_{l=0}^{L} M_l\, W_l, \qquad W_l \propto q_l^{\gamma_2}.$$

Here, $\gamma_2 = d + 2 \geq 3$ determines the cost of the deterministic dG solver. We then take the following iterative strategy, consisting of two main steps:

1. Optimal number of samples. We obtain the optimal number of samples in a similar way as MLMC:

$$M_l = \Big\lceil \big(\frac{\theta\,\varepsilon_{\text{TOL}}}{c_\alpha}\big)^{-2} \sqrt{\frac{V_l}{W_l}} \sum_{\ell=0}^{L} \sqrt{V_\ell\, W_\ell} \Big\rceil, \qquad W_l \propto q_l^{\gamma_2}. \tag{33}$$

2. Stopping criterion. We start with $L = 2$ and iteratively add levels until $\varepsilon_I \leq (1-\theta)\,\varepsilon_{\text{TOL}}$ is achieved. To find a practical stopping criterion, we start with (16) and assume that $|\mathbb{E}[\mathcal{Q}_l - \mathcal{Q}_{l-1}]| \approx c\,h^{\kappa_1\,q_L}$. We then have

$$\frac{|\mathbb{E}[\mathcal{Q}_l - \mathcal{Q}_{l-1}]|}{|\mathbb{E}[\mathcal{Q}_L - \mathcal{Q}_{L-1}]|} \approx \frac{h^{\kappa_1\,q_l}}{h^{\kappa_1\,q_L}} = h^{\kappa_1\,(q_l - q_L)} = h^{\kappa_1\,\beta\,(l-L)}.$$

Hence

$$\varepsilon_I = |\mathbb{E}[\mathcal{Q} - \mathcal{Q}_L]| \leq |\mathbb{E}[\mathcal{Q}_L - \mathcal{Q}_{L-1}]| \sum_{k=1}^{\infty} h^{k\,\kappa_1\,\beta} = \frac{h^{\kappa_1\,\beta}}{1 - h^{\kappa_1\,\beta}}\,|\mathbb{E}[\mathcal{Q}_L - \mathcal{Q}_{L-1}]|,$$

where the last equality follows from the geometrical series $\sum_{k=0}^{\infty}(\beta^{-q_1})^k = \frac{1}{1-h^{\kappa_1\,\beta}}$, since $h^{\kappa_1\,\beta} < 1$. Consequently, the condition we use to add levels in the numerical algorithm is

$$\max_{j\in\{0,1,2\}} \frac{h^{(j+1)\,\kappa_1\,\beta}}{1 - h^{\kappa_1\,\beta}}\,\big|\mathbb{E}[\mathcal{Q}_{L-j} - \mathcal{Q}_{L-j-1}]\big| \leq (1-\theta)\,\varepsilon_{\text{TOL}}. \tag{34}$$

This will ensure that the deterministic error approximated by an extrapolation form either of the three finest meshes is within the desired range.

Similar to the MLMC strategy, we approximate the variances $\{V_l\}_{l=0}^{L}$ in (33) by (18). When a new level L is added, the variance at the new level V_L cannot be approximated by (18), since the number of sample at the new level is not known. In this case, thanks to the strong error estimate (32), assuming $V_l = \mathbb{V}[\mathcal{Q}_l - \mathcal{Q}_{l-1}] \approx c\,h^{\kappa_2\,q_l}$, we first approximate V_L in terms of the variance at the previous level V_{L-1} by

$$V_L \approx h^{\kappa_2\,\beta}\,V_{L-1} \tag{35}$$

and then update the number of samples $\{M_l\}_{i=0}^{L}$ including the number of samples at the new level by (33). The expected values $\mathbb{E}[\mathcal{Q}_{L-j} - \mathcal{Q}_{L-j-1}]$ in (34), with $j = 1, 2, 3$, are also approximated by $\bar{G}_{L-j}$ in (18).

The MOMC algorithm is outlined in Algorithm 2.

LEMMA 2. *For every positive real number $r < 1$ and every positive integer $p \geq 1$, we have*

$$\sum_{l=0}^{\infty} r^{(q_0+\beta\,l)}\,(q_0 + \beta\,l)^p = \sum_{k=1}^{p} \tilde{c}_k\,r^k\,f^{(k)}(r), \qquad f(r) = \frac{r^{q_0}}{1-r^{\beta}}. \tag{36}$$

Proof. We start with the following geometrical series sum, thanks to $r^{\beta} < 1$:

$$\sum_{l=0}^{\infty}(r^{\beta})^l = \frac{1}{1-r^{\beta}}.$$

Hence

$$\sum_{l=0}^{\infty} r^{q_0+\beta\,l} = \frac{r^{q_0}}{1-r^{\beta}} =: f(r).$$

We differentiate the above formula with respect to r to obtain

$$\sum_{l=0}^{\infty}(q_0 + \beta\,l)\,r^{q_0+\beta\,l-1} = \frac{d}{dr}f(r).$$

Algorithm 2 MOMC algorithm

Start with $L = 2$, and generate an order hierarchy $\{q_l\}_{l=0}^{L}$ by (28).

Choose an initial set $\{M_l\}_{l=0}^{L}$ of samples.

loop

Approximate $\{V_l\}_{l=0}^{L}$ by (18).

Update the optimal number of samples $\{M_l\}_{l=0}^{L}$ by (33).

if (34) is satisfied

Compute $\mathcal{A}_{\text{MOMC}}$ by (29) and terminate the loop.

else

Set $L := L + 1$ and $q_L = q_0 + \beta\, L$.

Approximate V_L by (35) and compute $\{M_l\}_{l=0}^{L}$ by (33).

end if

end loop

We then multiply it by r to obtain

$$\sum_{l=0}^{\infty}(q_0 + \beta\, l)\, r^{q_0+\beta\, l} = r\, \frac{d}{dr} f(r).$$

We obtain (36) by repeating the above process, i.e. differentiate with respect to r and then multiply by r, p times. ∎

THEOREM 3. *Consider an order hierarchy $q_l = q_0 + \beta\, l$, with $l = 0, 1, \ldots, L$, where $q_0 \geq 1$ and $\beta \geq 1$ are cosntants. Let $\mathcal{Q}_l$ be the semi-discretization of $\mathcal{Q}$ by the q_l-th order dG method on a mesh with a fixed mesh size $h < 1$. If there are constants $c_1, c_2, c_3, \gamma_1, \gamma_2 > 0$ such that*

$$\begin{array}{lll} \textit{(A4)} & |\mathbb{E}[\mathcal{Q} - \mathcal{Q}_l]| \leq c_1\, h^{q_{1l}}, & q_{1l} = \kappa_1\, q_l, \quad \kappa_1\, q_0 \geq \gamma_1/2, \\ \textit{(A5)} & \mathbb{V}[\mathcal{Q} - \mathcal{Q}_l] \leq \mathbb{E}[|\mathcal{Q} - \mathcal{Q}_l|^2] \leq c_2\, h^{q_{2l}}, & q_{2l} = \kappa_2\, q_l, \quad \kappa_2\, q_0 > \gamma_1, \\ \textit{(A6)} & W_l \leq c_3\, h^{-\gamma_1}\, q_l^{\gamma_2}, & \end{array}$$

then, for any $\varepsilon_{TOL} < e^{-1}$, there exists an $L \in \mathbb{N}$ and a sequence $\{M_l\}_{l=0}^{L}$ such that the estimator $\mathcal{A}_{MOMC}$ has an error $\varepsilon_{MOMC} \lesssim \varepsilon_{TOL}$ with a computational cost proportional to ${\varepsilon_{TOL}}^{-2}$.

Proof. By writing $V_l = \mathbb{V}[\mathcal{Q}_l - \mathcal{Q}_{l-1}] = \mathbb{V}[\mathcal{Q} - \mathcal{Q}_{l-1}] - \mathbb{V}[\mathcal{Q} - \mathcal{Q}_l]$ and using the triangular inequality and *(A5)*, we get

$$V_l \leq c\, h^{q_{2l}}, \qquad c = c_2(1 + h^{-\kappa_2\beta} + 2\, h^{-\kappa_2\beta/2}). \tag{37}$$

Moreover, by minimizing $\mathbb{V}[\mathcal{A}_{\text{MOMC}}]$, or equivalently minimizing ε_{II}, for a fixed computational cost W_{MOMC}, we obtain from *(A6)* and (37):

$$M_l \propto \sqrt{V_l/W_l} \propto h^{(\gamma_1+q_{2l})/2}\, q_l^{-\gamma_2/2}. \tag{38}$$

We select L to be

$$L = \left\lceil \frac{\log(2c_1\, h^{\kappa_1\, q_0}\, {\varepsilon_{\text{TOL}}}^{-1})}{\log(h^{-\kappa_1\, \beta})} \right\rceil.$$

Hence

$$\frac{\log(2c_1\, h^{\kappa_1\, q_0}\, {\varepsilon_{\text{TOL}}}^{-1})}{\log(h^{-\kappa_1\, \beta})} \leq L < \frac{\log(2c_1\, h^{\kappa_1\, q_0}\, {\varepsilon_{\text{TOL}}}^{-1})}{\log(h^{-\kappa_1\, \beta})} + 1.$$

By the rules of logarithms and simple algebraic manipulations, we get

$$\frac{1}{2}\, \varepsilon_{\text{TOL}}\, h^{\kappa_1\, \beta} < c_1\, h^{\kappa_1\, q_L} \leq \frac{1}{2}\, \varepsilon_{\text{TOL}}. \tag{39}$$

By the right inequality in (39) and *(A4)*, the deterministic error is bounded by

$$\varepsilon_I \leq \frac{1}{2}\, \varepsilon_{\text{TOL}}. \tag{40}$$

By the left inequality in (39), we have

$$h^{-\kappa_1\, q_L} < 2\, c_1\, h^{-\kappa_1\, \beta}\, {\varepsilon_{\text{TOL}}}^{-1},$$

and hence by taking logarithm and rearranging we obtain

$$q_L < \frac{\log(2\, c_1\, h^{-\kappa_1\, \beta})}{\log(h^{-\kappa_1})} + \frac{1}{\log(h^{-\kappa_1})}\, \log\left({\varepsilon_{\text{TOL}}}^{-1}\right) =: \hat{c}_1 + \hat{c}_2\, \log\left({\varepsilon_{\text{TOL}}}^{-1}\right),$$

where the constants $\hat{c}_1$ and $\hat{c}_2$ are independent of ε_{TOL} and L. The right hand side of the above inequality is a logarithmic growth and can be bounded by an algebraic growth. In particular, there exists a constant $\hat{c}$ such that

$$\hat{c}_1 + \hat{c}_2\, \log\left({\varepsilon_{\text{TOL}}}^{-1}\right) < \hat{c}\, {\varepsilon_{\text{TOL}}}^{-2/(\gamma_2+1)},$$

and hence

$$q_L < \hat{c}\, {\varepsilon_{\text{TOL}}}^{-2/(\gamma_2+1)}.$$

We therefore have

$$\sum_{l=0}^{L} q_l^{\gamma_2} < (L+1)\, q_L^{\gamma_2} < q_L^{\gamma_2+1} < \hat{c}^{\gamma_2+1}\, {\varepsilon_{\text{TOL}}}^{-2}. \tag{41}$$

Now, motivated by (38), we set

$$M_l = \left\lceil 4\, {\varepsilon_{\text{TOL}}}^{-2}\, c\, c_\alpha^2\, S\, h^{(\gamma_1+\kappa_2\, q_l)/2}\, q_l^{-\gamma_2/2} \right\rceil, \tag{42}$$

where

$$S = h^{-\gamma_1/2} \sum_{k=1}^{\lceil \gamma_2/2 \rceil} \tilde{c}_k\, h^{k\, \kappa_2/2}\, f^{(k)}(r), \qquad f(r) = \frac{r^{q_0}}{1-r^\beta}, \qquad r = h^{\kappa_2/2} < 1.$$

From (42) we get

$$\frac{c\, c_\alpha^2}{M_l} \leq \frac{1}{4}\, {\varepsilon_{\text{TOL}}}^2\, S^{-1}\, h^{-(\gamma_1+\kappa_2\, q_l)/2}\, q_l^{\gamma_2/2}.$$

Then, by (37) we have

$$c_\alpha^2 \sum_{l=0}^{L} \frac{V_l}{M_l} \leq \sum_{l=0}^{L} \frac{c\, c_\alpha^2}{M_l} h^{\kappa_2\, q_l} \leq \frac{1}{4}\, {\varepsilon_{\text{TOL}}}^2\, S^{-1} \sum_{l=0}^{L} h^{(\kappa_2\, q_l - \gamma_1)/2}\, q_l^{\gamma_2/2}.$$

Moreover, by Lemma 2 with $r := h^{\kappa_2/2} < 1$ and $p := \lceil \gamma_2/2 \rceil > 1$, we have

$$\sum_{l=0}^{L} h^{(\kappa_2\, q_l - \gamma_1)/2}\, q_l^{\gamma_2/2} < h^{-\gamma_1/2} \sum_{l=0}^{\infty} h^{\kappa_2\, (q_0 + \beta\, l)/2}\, (q_0 + \beta\, l)^{\lceil \gamma_2/2 \rceil} < S. \tag{43}$$

Hence, the statistical error is bounded by

$$\varepsilon_{II} \lesssim c_\alpha \sqrt{\sum_{l=0}^{L} \frac{V_l}{M_l}} \leq \frac{1}{2}\, \varepsilon_{\text{TOL}}. \tag{44}$$

By (40) and (44), the total error reads $\varepsilon_{\text{MOMC}} \lesssim \varepsilon_{\text{TOL}}$. It is left to show that the computational cost is proportional to ${\varepsilon_{\text{TOL}}}^{-2}$. By (42), we have

$$M_l < 4\, {\varepsilon_{\text{TOL}}}^{-2}\, c\, c_\alpha^2\, S\, h^{(\gamma_1 + \kappa_2\, q_l)/2}\, q_l^{-\gamma_2/2} + 1.$$

Hence, by *(A6)*, the computational cost reads

$$\begin{aligned} W_{\text{MOMC}} &= \sum_{l=0}^{L} M_l\, W_l \leq c_3 \sum_{l=0}^{L} M_l\, h^{-\gamma_1}\, q_l^{\gamma_2} \\ &< 4\, c_3\, {\varepsilon_{\text{TOL}}}^{-2}\, c\, c_\alpha^2\, S \sum_{l=0}^{L} h^{(\kappa_2\, q_l - \gamma_1)/2}\, q_l^{\gamma_2/2} + c_3\, h^{-\gamma_1} \sum_{l=0}^{L} q_l^{\gamma_2}. \end{aligned}$$

By (43) we obtain

$$W_{\text{MOMC}} < c_{\text{W}}\, {\varepsilon_{\text{TOL}}}^{-2}, \qquad c_{\text{W}} = 4\, c_3\, c\, c_\alpha^2\, S^2 + c_3\, \hat{c}^{\gamma_2 + 1}\, h^{-\gamma_1}.$$

This completes the proof. ∎

REMARK 1. *Theorems 1 and 3 show that, under the same accuracy constraint ($\varepsilon_{MLMC} \lesssim \varepsilon_{TOL}$ and $\varepsilon_{MOMC} \lesssim \varepsilon_{TOL}$), the total computational cost of both MLMC and MOMC is proportional to ${\varepsilon_{TOL}}^{-2}$. This verifies that MOMC is a valid alternative to MLMC for hyperbolic problems. In addition, we will present numerical evidence (see Figures 1 and 4) that the multi-order approach is faster than the mesh-based multi-level approach for waves that traverse long distances. This superiority of MOMC over MLMC is due to the advantage of high-order schemes in controlling dispersive errors in wave propagation problems. In principle, this claim can be made rigorous by carefully tracking the the effects of dispersive errors on the constant c_W, which appears in the computational cost. Such analysis is the topic of future work.*

6. Numerical examples. In this section we present numerical results from problems in (1+1) and (2+1) dimensions demonstrating the performance of the two methods described above. The first example considers the scalar wave equation, and the second example considers the elastic wave equation. For the details of the dG deterministic solver, we refer to [2, 3].

6.1. Example 1. We first consider the scalar wave equation in (1+1) dimensions on the domain $D = [0, 10]$ and with a potential energy density $G(x) = (c(x)u_x)^2/2$. We take the initial data to be

$$u(x, 0) = e^{-(x-5)^2}, \quad v(x, 0) = 0,$$

and impose homogenous Dirichlet conditions on both boundaries. Here the square of the wave speed is assumed to be uncertain in the x direction and modeled by 10 independent and uniformly distributed random variables $y_i = U[0, 1]$. Precisely the piecewise constant wave speed is

$$c^2(x, \mathbf{y}) = 1 + \frac{y_i}{100}, \quad x \in [i - 1, i], \quad i = 1, \ldots, 10.$$

We perform the simulations by starting both methods on a uniform grid conforming with the wave speed. In MLMC we choose the base element size is $h_0 = 1$ with the fixed order $q = 4$, and in MOMC we choose the fixed mesh size $h = 1$ and start with the order $q_0 = 4$, corresponding to a fourth order space-time accurate method in the displacement u.

The quantity of interest is

$$\mathcal{Q}(\mathbf{y}) = \left(\int_D |u(T, x, \mathbf{y})|^2 \, dx \right)^{\frac{1}{2}},$$

where T is the final time and the integral in x is approximated by sufficiently accurate Gauss-Legendre-Lobatto quadrature.

The parameters in MOMC are $(\gamma_2, \kappa_1, \kappa_2) = (2, 1, 2)$ and the parameters in MLMC are $(\gamma_1, q_1, q_2) = (2, 4, 8)$. For MLMC we set $\beta = 2$ and for MOMC we present results for $\beta = 1$ and 2. For both methods we set $\theta = 1/2$ and $c_\alpha = 1.96$.

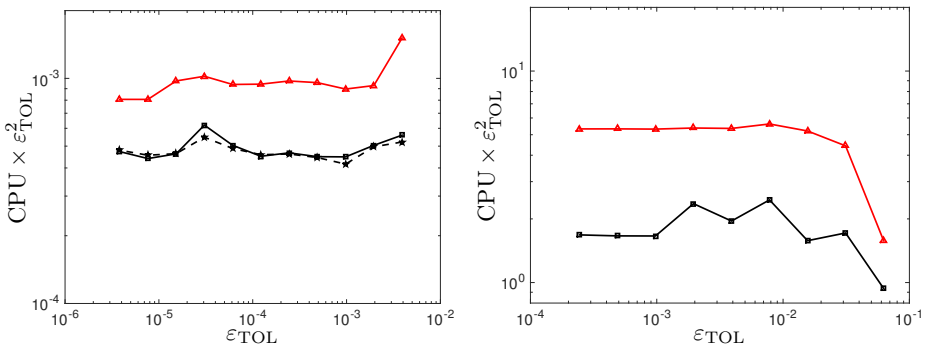

FIG. 1. *Product of CPU time and the square of the tolerance. The red curves with triangles represents MLMC and the black curves with squares represents MOMC with $\beta = 2$ and the dashed line MOMC with $\beta = 1$. The left figure is for $T = 20$ and the right is for $T = 200$. For this problem MOMC uses abut 1.8 and 3.2 times less CPU-time to reach a given tolerance.*

To illustrate the advantage of using MOMC we consider two final simulation times. First we set $T = 20$ and perform simulations with tolerances $\varepsilon_{\text{TOL}} = 2^{-8-s}$, $s = 0, \ldots, 10$. These simulations are performed three times with different random seeds. In a second set of simulations we increase the final time to $T = 200$ and perform simulations with tolerances $\varepsilon_{\text{TOL}} = 2^{-7-s}$, $s = 0, \ldots, 5$. For the second set of simulations we only present results for $\beta = 2$ for MOMC.

To confirm the complexity results of Theorem 1 and 3 we plot the product of the square of the tolerance and total CPU time as a function of tolerance. The results for both final times can be found in Figure 1. As can be seen to the left in Figure 1, for the short time $T = 20$, MOMC is about 1.8 times faster than MLMC for both choices of β in MOMC. For the longer simulation time we find that MOMC is about 3.2 times faster than MLMC.

For the short time simulation we also report the distributions of the number of samples per level for the three different methods and for the different tolerances. As can be seen in Figure 2, at higher levels, where the deterministic solver per sample is computationally costly, the number of samples (or the number of the deterministic solves) are much smaller than the number of samples at lower levels, where the deterministic solver per sample is computationally cheap. This intuitively show why MLMC and MOMC work.

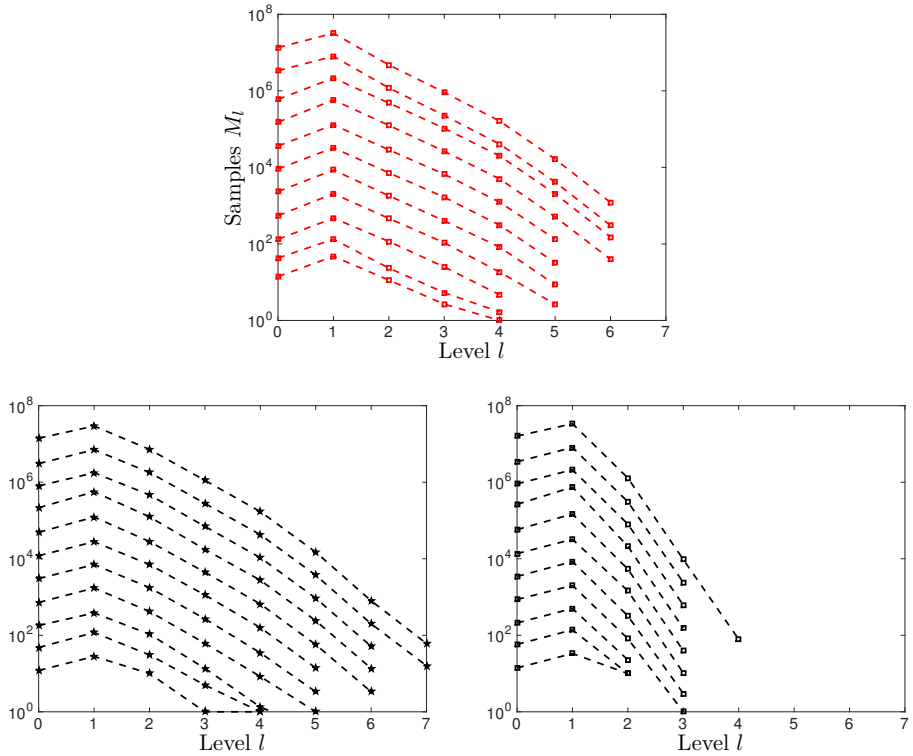

FIG. 2. *Number of samples per level for different tolerances* $\varepsilon_{\mathrm{TOL}} = 2^{-8-s}$, $s = 0, \ldots, 10$. *In each figure, the strictest tolerance corresponds to the curve with the highest number of samples. The number of samples are monotonically decreasing as the tolerance is relaxed. On top MLMC, bottom left MOMC with* $\beta = 1$, *and bottom right MOMC with* $\beta = 2$.

6.2. Example 2. In this example we consider the elastic wave equation with traction free boundary conditions on the domain $D = (x_1, x_2) \in [-1, 1] \times [-2, 2]$. In MLMC, the domain D is discretized with square elements with sides $h_l = h_0 \beta^{-l}$, with $\beta = 2$ and $h_0 = \frac{1}{2}$, and we use dG with the fixed order $q = 4$. In MOMC we choose the fixed mesh size $h = 1/2$ and start with the order $q_0 = 4$. The material properties are taken to be piecewise constant but different above and below $x_2 = 0$, precisely

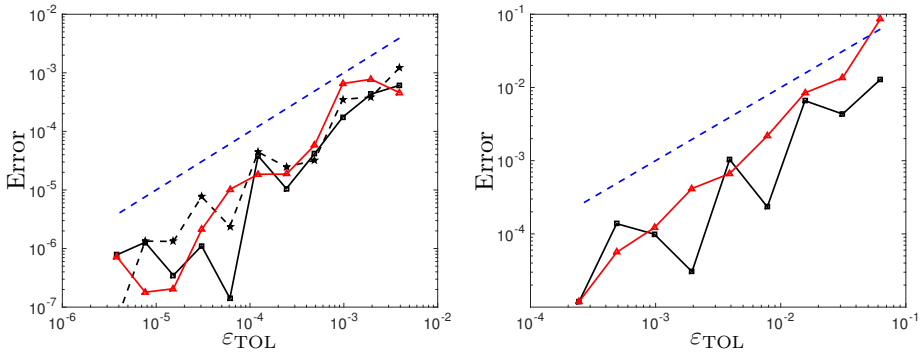

FIG. 3. *Verification that the tolerance is met. Plotted is the error as a function of the tolerance for MLMC (solid red with triangles), MOMC and $\beta = 1$ (dashed black with pentagrams) and MOMC and $\beta = 2$ (solid black with squares). The left figure is for $T = 20$ and the right is for $T = 200$.*

they are

$$(\rho, \lambda, \mu) = \begin{cases} (1, 4, 1 + y_1) & x_2 > 0, \\ (1, 4, 1 + y_2) & x_2 < 0, \end{cases} \tag{45}$$

where y_1 and y_2 are uniform random variables on $[0, 1]$. Note that the grid coincides with the material interface at $x_2 = 0$, so that the order of the dG method is not affected by the jump discontinuity in μ. The initial data is chosen to be

$$u_1 = e^{-6((x_1-0.15)^2+(x_2-0.1)^2)}, \quad u_2 = e^{-6((x_1-0.12)^2+(x_2-0.14)^2)}, \quad v_1 = v_2 = 0.$$

Here u_1 and u_2 are the displacements and v_1 and v_2 are the velocities.

The quantity of interest is

$$Q(y) = \left(\int_D u_1(T, \mathbf{x}, \mathbf{y})^2 + u_2(T, \mathbf{x}, \mathbf{y})^2 \, d\mathbf{x} \right)^{\frac{1}{2}},$$

where T is the final time of the simulation.

We present results for three different final times $T = 1, 10$ and 100. In Figure 4 we plot the product of the square of the tolerance and total CPU time as a function of tolerance for the three different final times. The results are for MOMC with $(\gamma_2, \kappa_1, \kappa_2) = (4, 1, 2)$ and $\beta = 1$ and for MLMC with $(\gamma_1, q_1, q_2) = (3, 4, 8)$ and $\beta = 2$. For both methods we set $\theta = 1/2$ and $c_\alpha = 1.96$.

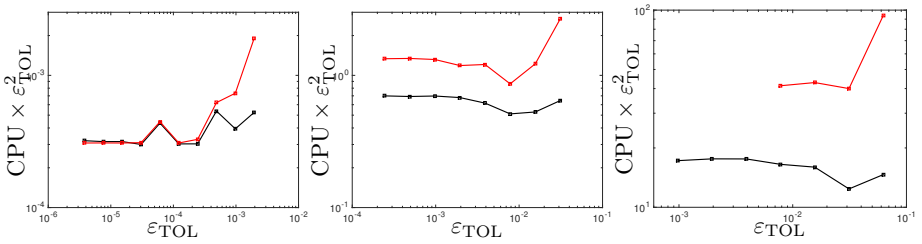

FIG. 4. *From left to right $T = 1, 10, 100$. MLMC (red), MOMC with $\beta = 1$ (black).*

As in the previous example, as the final time becomes longer the advantage of the MOMC method becomes more pronounced. In this case the computational time

is about the same when $T = 1$, about 1.9 times faster when $T = 10$ and 2.4 times faster when $T = 100$. Again we find that the tolerance is met for both the methods and for all the final times, see Figure 5.

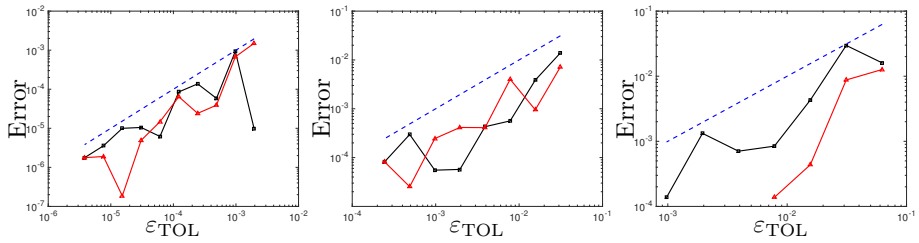

FIG. 5. *Verification that the tolerance is met. From left to right* $T = 1, 10, 100$. *MLMC (red), MOMC with* $\beta = 1$ *(black).*

7. Conclusion. We presented the multi-order Monte Carlo method for forward propagation of uncertainties in hyperbolic problems. Here the method used an arbitrary order energy-based discontinuous Galerkin discretization to build order hierarchies but we note that the MOMC method could of course also use any suitable discretization capable of discretization at arbitrary order. In fact, the complexity theorems we have presented do not rely on the dG method but are general in that they accept any discretization.

We found that the optimal complexity of the original MLMC method also carries over to our multi-order Monte Carlo method and that the new method is faster when the problem at hand requires propagation of waves over long distances. Another feature of the MOMC is that a single mesh can be generated, something that may be of practical importance both for increased set-up time as well as for the ability to load balance parallel computations once and for all in the beginning of a simulation.

Our method illustrates the power of the multi-level Monte Carlo framework and how easily it can be adopted and extended. We are currently exploring extensions of the MOMC method to other hyperbolic problems and more realistic applications and we are also working on extending it to the *hp*-refinement regime.

REFERENCES

[1] D. Appelö and T. Hagstrom, *dg-DATH: Discontinuous Galerkin Solver by Daniel Appelo & Thomas Hagstrom for the Elastic Wave Equation*, 2015, https://bitbucket.org/appelo/dg_dath_elastic_v1.0.

[2] D. Appelö and T. Hagstrom, *An energy-based discontinuous Galerkin discretization of the elastic wave equation in second order form*, Computer Methods in Applied Mechanics and Engineering, xxx (2016), p. xxx.

[3] D. Appelö and T. Hagstrom, *A new discontinuous Galerkin formulation for wave equations in second order form*, Siam Journal On Numerical Analysis, 53 (2016), pp. 2705–2726.

[4] I. Babuška, M. Motamed, and R. Tempone, *A stochastic multiscale method for the elastodynamic wave equations arising from fiber composites*, Computer Methods in Applied Mechanics and Engineering, 276 (2014), pp. 190–211.

[5] A. Barth, C. Schwab, and N. Zollinger, *Multilevel Monte Carlo finite element method for elliptic PDEs with stochastic coefficients*, Numer. Math., 199 (2011), pp. 123–161.

[6] K. A. Cliffe, M. B. Giles, R. Scheichl, and A. L. Teckentrup, *Multilevel Monte Carlo methods and applications to elliptic PDEs with random coefficients*, Comput. Visual Sci., 14 (2011), pp. 3–15.

[7] N. Collier, A.-L. Haji-Ali, F. Nobile, E. von Schwerin, and R. Tempone, *A continuation multilevel Monte Carlo algorithm*, BIT Numer. Math., (2014). (in press).

[8] G. S. Fishman, *Monte Carlo: Concepts, Algorithms, and Applications*, Springer- Verlag, New York, 1996.
[9] R. G. Ghanem and P. D. Spanos, *Stochastic finite elements: A spectral approach*, Springer, New York, 1991.
[10] M. B. Giles, *Multilevel Monte Carlo path simulation*, Oper. Res., 56 (2008), pp. 607–617.
[11] A.-L. Haji-Ali, F. Nobile, and R. Tempone, *Multi-index Monte Carlo: when sparsity meets sampling*, Numerische Mathematik, (2015).
[12] T. Y. Hou and X. Wu, *Quasi-Monte Carlo methods for elliptic PDEs with random coefficients and applications*, J. Comput. Phys., 230 (2011), pp. 3668–3694.
[13] F. Y. Kuo, C. Schwab, and I. H. Sloan, *Multi-level quasi-Monte Carlo finite element methods for a class of elliptic PDEs with random coefficients*, Foundations of Computational Mathematics, 15 (2015), pp. 411–449.
[14] S. Mishra and C. Schwab, *Sparse tensor multi-level Monte Carlo finite volume methods hyperbolic conservation laws with random initial data*, Mathematics of computation, 81 (2012), pp. 1979–2018.
[15] M. Motamed, F. Nobile, and R. Tempone, *A stochastic collocation method for the second order wave equation with a discontinuous random speed*, Numer. Math., 123 (2013), pp. 493–536.
[16] M. Motamed, F. Nobile, and R. Tempone, *Analysis and computation of the elastic wave equation with random coefficients*, Computers and Mathematics with Applications, 70 (2015), pp. 2454–2473.
[17] F. Nobile, R. Tempone, and C. G. Webster, *A sparse grid stochastic collocation method for partial differential equations with random input data*, SIAM J. Numer. Anal., 46 (2008), pp. 2309–2345.
[18] J. Sukys, S. Mishra, and C. Schwab, *Multi-level Monte Carlo finite difference and finite volume methods for stochastic linear hyperbolic systems*, in Monte Carlo and Quasi-Monte Carlo Methods, J. Dick, F. Y. Kuo, G. W. Peters, and I. H. Sloan, eds., vol. 65 of Springer Proceedings in Mathematics and Statistics, Springer, 2012, pp. 649–666.
[19] D. Xiu and J. S. Hesthaven, *High-order collocation methods for differential equations with random inputs*, SIAM J. Sci. Comput., 27 (2005), pp. 1118–1139.